COMPARISON OF LAND COVER MAPS USING HIGH RESOLUTION MULTISPECTRAL AND HYPERSPECTRAL IMAGERY

J. Marcello, D. Rodríguez-Esparragón, D. Moreno

Instituto de Oceanografía y Cambio Global, IOCAG. Universidad de Las Palmas de Gran Canaria, ULPGC. Parque Científico Tecnológico Marino de Taliarte, s/n, 35214, Telde, Las Palmas, Spain.
E–mails: javier.marcello@ulpgc.es, dionisio.rodriguez@ulpgc.es, juan.moreno114@alu.ulpgc.es

ABSTRACT

Land cover information is a fundamental parameter in a wide range of applications like urban growth, land degradation, climate change, food security, environmental sustainability, etc. In this context, remote sensing satellites can provide valuable data to allow the generation of thematic maps. On the other hand, the recent availability of hyperspectral sensors on board aircrafts and drones offers an opportunity to improve the resolution and accuracy of land cover maps. In island territories, where land is usually a scarce resource, the need of very high spatial resolution (VHR) is essential. In this context, we have generated VHR land cover maps using multispectral Worldview data and hyperspectral airborne CASI information. In particular, after corrections and pansharpening enhancements, we have analyzed pixel-based and object-based classification approaches using different input band combinations. We have compared the performance when using multispectral or hyperspectral imagery and its robustness depending on the quality of the training samples considered.

Index Terms— Land use land cover, OBIA classification, support vector machines, hyperspectral, CASI.

1. INTRODUCTION

Land use and land cover information are essential for many applications, such as urban and land management and planning, climatic and ecological research, etc. This importance is more relevant in island areas where land is usually scarcer and a good management and planning are important and have to be compatible with relevant economic activities, like tourism for example.

The methodological procedures for the generation of land use and land cover (LULC) maps require a high degree of human intervention, since they are almost entirely based on the photointerpretation of imagery. However, recent improvements in the quality of sensors have meant a significant increase in the availability of high resolution images. Thus, the use of very high resolution (VHR) remote sensing data can be an essential solution to derive such information. In this context, to generate detailed LULC maps, VHR data can be acquired from multispectral satellite sensors. However, nowadays, hyperspectral VHR sensors are not yet operational onboard satellites. In consequence, only airborne or drone systems can provide such level of spatial detail.

In any case, the multispectral or hyperspectral data recorded must be processed in order to remove distortions and to generate the desired thematic maps. In particular, improvements in classification accuracy are an important concern in remote sensing [1, 2] and a significant research has been conducted in order to generate reliable land cover maps, specifically using VHR data.

The main objective of this work is to quantify the improvement in the VHR maps generated by the use of hyperspectral imagery with respect to multispectral for the same spatial resolution. In addition, a comprehensive study of different combinations of common input features has been carried out in order to identify the most accurate and robust classification methodology to derive land cover maps. Finally, an assessment of the effects of the quality and quantity of the training data is also performed.

2. MAPPING METHODOLOGY

2.1. Area of Study

The Natural Reserve of Maspalomas (Gran Canaria Island, Spain) encompasses an area of 403.9 hectares of sand dunes and includes a small lagoon of great ecological value as well as a bird nesting zone. It was a well preserved ecosystem and the area remained largely unspoiled until the 1960s, when large scale tourist development changed the area. In fact, it is the most famous holiday resort in Gran Canaria with more than 2 million visitors each year and plenty of hotels, apartments, commercial centers, golf courses, etc.

2.2. Data

The CASI 1500i is a hyperspectral visible near infrared (VNIR) push-broom imager which measures the incoming

radiance along up to 1500 spatial pixels "across-track" in up to 288 separate spectral bands. The spectral bands can be placed within the 380 to 1050 nm spectral range. The band-to-band distance between spectral rows is 2.4 nm, while the bandwidth of each spectral row is around 3 nm. Incoming radiation is stored in 14 bits per sample [3].

In our selected configuration for the Maspalomas campaign, the INTA CASI airborne sensor was installed in the CASA C-2012-200 aircraft. The spectral resolution was reduced to 68 bands to increase the signal-to-noise ratio, as the required spatial resolution was 50 cm.

A Worldview-2 (WV-2) ortho-ready image of the Maspalomas area was used in the study. Its sensor has a radiometric resolution of 11 bits and a spatial resolution, at nadir, of 1.8 m and 0.46 m for the multispectral (MS) and panchromatic (PAN) bands, respectively. The eight MS bands range from 400 to 1040 nm.

Figure 1 includes the Worldview-2 and CASI color composite imagery used in the analysis.

2.3. Land cover classes

A total of 12 classes were considered in the analysis: trees, shrubs, grass, sand, bare soil, built soil, asphalt, swimming pools, lake, sea, waves and others. Different sets of training and test regions (ROIs) for each sensor, based on ground information knowledge and using a random sampling strategy, were used during the classification. Specifically, 4 different training ROIs were considered including only pure pixels, mixed pixels (close to the edge of each object) and two of them containing a combination of both types of pixels. Special care was taken into account when selecting training and test regions to guarantee that they were correct and applicable for both datasets used in the analysis and that they included the possible variability of each cover within the image.

2.4. Methodology

The overall processing and evaluation approach to generate the land cover maps is next presented, where different inputs to the classification algorithm were analyzed in order to select the best methodology.

First, the corresponding preprocessing algorithms were applied to the images. In particular, geometric, radiometric and atmospheric corrections, using ATCOR 4 [3] for CASI and FLAASH [4] for WV-2, were done. Both datasets were subsequently co-registered by means of a large set of distributed ground control points to allow the accurate use of the train and test regions and a change detection analysis. In addition, for the Worldview-2 image, the pan-sharpening process was applied using the weighted wavelet 'à trous' method through fractal dimension maps algorithm [5, 6] to increase the spatial resolution to the CASI pixel size with minimum spectral distortion.

(a)

(b)

Figure 1. True color composite images: (a) Worldview-2 of June 4, 2015 and (b) CASI 1500i of June 2, 2017.

Secondly, the corrected images were subjected to a feature extraction stage. In this way, in addition to the spectral channels, the inclusion of additional information was considered. Features analyzed were the optimal components after PCA (Principal Component Analysis) and MNF (Minimum Noise Fraction) transforms [7] and the texture information (mean, variance and entropy) from the co-occurrence filter applied to the first principal component. An important approach to extract relevant information, mainly in hyperspectral imagery, is also the application of linear unmixing techniques [8]. Unmixing consists on estimating the contribution percentage of each pure class (endmember) to the total reflectivity of each pixel. There are several strategies for the extraction of endmembers, although in this analysis the spectral information from the training regions, obtained from the CASI image itself, has been used. In this context, abundance maps corresponding to each class of interest have been derived from the spectral channels of each sensor.

Finally, the spectral bands and the resulting features (PCA and MNF components, texture bands and abundance maps) were used as input data to the classifier. Pixel level and object based (OBIA) classification were tested.

In traditional pixel-based classification, pixels are classified individually according to their digital values. On the other hand, the object-based image analysis is a more efficient classification approach when dealing with very high resolution data. The main step in OBIA is the segmentation of the image followed by successive analyses, sometimes at

different hierarchical levels in order to create relationships within segments or objects. After the segmentation process, the image is divided into homogeneous regions according to several parameters (band weights, scale, color, shape, texture, etc.) defined by the operator, with the objective of creating appropriate object delimiting borders. We applied an algorithm based on watershed segmentation and merging stages [9]. As soon as a suitable segmentation is obtained, the classifier is applied. Figure 2 shows an example of the segmentation obtained in a small portion of the CASI image.

After the analysis of literature and the assessment of various classifiers, Support Vector Machine (SVM) has been selected [10, 11]. Even though more advanced classifier exist, in [11] a recent comparison of advanced methods (SVMs, RFs, neural networks, deep CNNs, logistic regression-based techniques, and sparse representation-based classifiers) demonstrates that SVM is widely used because of its accuracy, stability, automation and simplicity; being less sensitive to the dimensionality of the data and to the quantity and quality of the training regions. The appropriate parameterization has been used, selecting the radial base function kernel and the optimal parameters (C, ɣ) using coarse and fine grid search techniques [12].

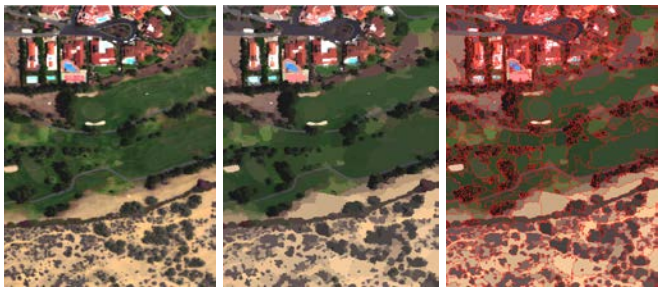

(a) (b) (c)

Figure 2. CASI image: (a) true color composite, (b) segmented image displaying the mean value of each object and (c) segmented image overlaying the object contours.

As usual, to evaluate the accuracy of the thematic maps obtained, using a different set of ground-truth regions, the confusion matrix, its derived metrics and the Kappa coefficient have been used [1].

4. RESULTS

As indicated, SVM was applied to the corrected and enhanced VHR multispectral and hyperspectral data, analyzing the following input combinations:

- Spectral bands.
- PCA components (after visual analysis of each eigenvector, the first 10 principal components were selected for CASI).
- MNF components (the 25 first components were selected for CASI).
- Spectral bands plus texture information.
- Abundance maps (Ab) of each class after the application of linear unmixing techniques to the bands or to the best dimensionality reduction components.

As indicated, to assess the robustness of the different methodologies to the quality of the training information, 4 different training regions were considered. Table 1 includes the overall accuracy of each of the strategies evaluated.

Table 1. SVM overall accuracy (%) for the CASI and WV-2 data (best in bold and number of bands in brackets).

Input (# bands)	Pure	Mixed	P+M 1	P+M 2
CASI Pixel-based				
Pixel-based: - Spectral bands (68)	85.47	76.35	91.39	91.91
- PCA 1-10 (10)	85.40	76.19	91.23	92.16
- MNF 1-25 (25)	**87.84**	80.36	91.35	91.35
- Bands + texture (71)	86.29	73.83	**91.53**	**92.38**
- Ab bands (12)	56.43	53.67	63.17	61.27
- Ab PCA 1-10 (12)	45.34	45.03	60.75	50.26
- Ab MNF 1-25 (12)	62.21	56.61	64.44	62.16
CASI Object-based				
Spectral bands (68)	86.18	**80.61**	90.55	91.71
WV-2 Pixel-based				
Spectral bands (8)	**87.54**	71.71	**88.57**	**90.14**
Bands + texture (11)	87.20	70.49	87.52	88.60
WV-2 Object-based				
Spectral bands (8)	**87.54**	**77.73**	87.89	89.69

With respect to the sensors, we can appreciate that CASI provides slightly better accuracies than WV-2 but, at least for this application where most of classes are spectrally not too similar, hyperspectral data is not offering a significant improvement. With respect to the training ROIs, better accuracies are achieved using regions that combine pure and mixed pixels. Regarding the dimensionality reduction techniques to alleviate the Hughes effect, MNF performs better than PCA for the HS imagery. Texture information is not always improving the performance of the methodology but its inclusion in the CASI data is providing good results. The use of unmixing techniques prior to the classification is not improving the accuracy, even when dealing with hyperspectral imagery. We also tested the application of a median filter to the abundance maps to get better results and a 20% increase in accuracy is, in general, gained. Finally, OBIA only provides superior performance than pixel-based methods in some specific cases; thus, more testing with different segmentations has to be performed.

Figure 3 shows the best land cover maps for each sensor; both obtained using the training ROI combining pure and mixed pixels. Results are similar with overall accuracies of 92.38% and 90.14% for CASI and WV-2, respectively.

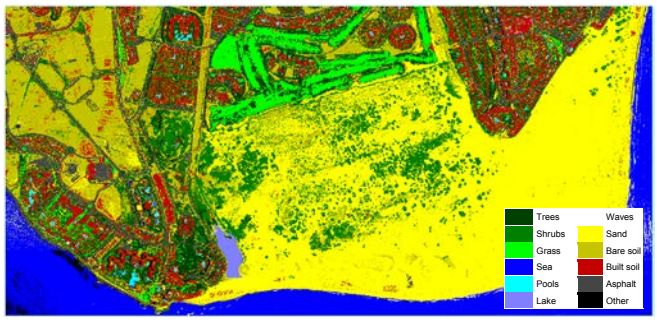

(a)

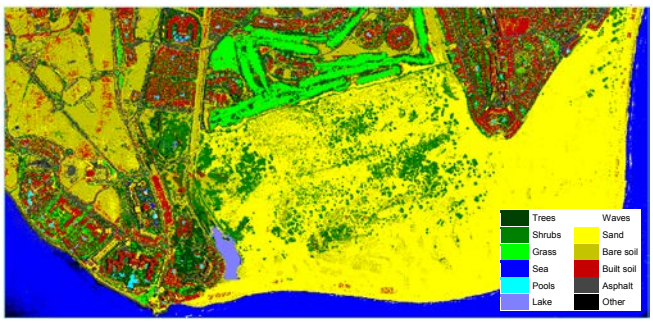

(b)

Figure 3. Best land cover maps: (a) CASI and (b) WV-2.

5. CONCLUSIONS

This work has analyzed different methodologies for the generation of land cover maps in the area of Maspalomas (Gran Canaria, Spain). Two very high resolution images have been used, one from the CASI hyperspectral airborne sensor and another from the multispectral WorldView-2 satellite, both imagery recorded during the month of June

After applying the corresponding geometric, radiometric and atmospheric corrections and, specifically the pansharpening in the satellite image to improve its spatial resolution, the accuracy of the SVM classification algorithm has been assessed, both at pixel and object levels, when applied to different input combinations (spectral bands, PCA and MNF components and texture information). In addition, abundances obtained from the linear unmixing algorithm were included in the study.

The best methodology, using widespread feature extraction and classification techniques, has been identified for each sensor and excellent performances have been achieved.

6. ACKNOWLEDGEMENTS

This research has been supported by the ARTEMISAT-2 (CTM2016-77733-R) project, funded by the Spanish *Agencia Estatal de Invetigación* (AEI) and by the *Fondo Europeo de Desarrollo Regional* (FEDER). Authors want to acknowledge INTA (*Instituto Nacional de Técnica Aeroespacial*) for providing the CASI imagery

7. REFERENCES

[1] Tso, B. and P.M. Mather, *Classification Methods for Remotely Sensed Data*, Taylor and Francis Inc., New York, 2009.

[2] M. Li, S. Zhang, B. Zhang, S. Li and C. Wu, "A review of remote sensing image classification technique: the role of spatio-contextual information," *European Journal of Remote Sensing*, 47, pp. 389-411, 2014.

[3] E. de Miguel, A. Fernández-Renau, E. Prado, M. Jiménez, O. Gutiérrez, C. Linés, J. Gómez, A.I. Martín. and F. Muñoz, "The processing of CASI-1500i data at INTA PAF," *EARSeL eProceedings*, 13(1), pp. 20-29, 2014.

[4] Vermote E., D. Tanré, J.L. Deuzé, M. Herman, J.J. Morcrette and S.Y. Kotchenova, *Second Simulation of a Satellite Signal in the Solar Spectrum – Vector* (*6SV*), 6S User Guide v.3, NASA Goddard Space Flight Center, Greenbelt, MD, 2006.

[5] M. Lillo-Saavedra and C. Gonzalo-Martin, "Spectral or spatial quality for fused satellite imagery? A trade-off solution using the wavelet à trous algorithm," *Int. J. Remote Sensing,* 6(27), pp. 1453–146. 2006.

[6] E. Ibarrola-Ulzurrun, C. Gonzalo-Martin and J. Marcello, "Fusion of High Resolution Multispectral Imagery in Vulnerable Coastal and Land Ecosystems," *Sensors*, 17(2), 228, 2017.

[7] E. Ibarrola-Ulzurrun, J. Marcello and C Gonzalo-Martin, "Assessment of Component Selection Strategies in Hyperspectral Imagery," *Entropy*, 19(12), 666, 2017.

[8] J. Bioucas, A. Plaza, N. Dobigeon, M. Parente, Q. Du, P. Gader and J. Chanussot, "Hyperspectral unmixing overview: Geometrical, statistical, and sparse regression-based approaches," *IEEE J. Select. Topics Applied Earth Observation and Remote Sensing*, 5(2), pp. 354–379, 2012.

[9] Jin, X., *Segmentation-based image processing system*, US Patent 8,260,048, 2012.

[10] U. Maulik and D. Chakraborty, "Remote Sensing Image Classification: A survey of support-vector-machine-based advanced techniques," *IEEE Geoscience and Remote Sensing Magazine*, 5(1), pp. 33-52, 2017.

[11] P. Ghamisi, J. Plaza, Y. Chen, J. Li and A. Plaza, "Advanced spectral classifiers for hyperspectral images," *IEEE Geosciences and Remote Sensing Magazine*, pp. 8-32, march 2017.

[12] X. Yang, "Parameterizing Support Vector Machines for Land Cover Classification," *Photogrammetric Engineering and Remote Sensing*, 77(1), pp. 27-37, 2011.

[13] W. Liao. J. Chanussot, M. Dalla Mura, X. Huang, R. Bellens, S. Gautama and W. Philips, "Taking Optimal Advantage of Fine Spatial Resolution: Promoting partial image reconstruction for the morphological analysis of very-high-resolution images," *IEEE Geosciences and Remote Sensing Magazine*, 2, pp. 8-28, 2017.